



## Use of 3-D modeling in the early development phase of pectin tablets.

Linda Salbu<sup>a</sup>, Katharina M. Picker-Freyer<sup>b</sup>, Wolfgang Schmid<sup>b</sup>, Annette Bauer-Brandl<sup>a,c</sup>, Ingunn Tho<sup>a\*</sup>

<sup>a</sup>University of Tromsø, Department of Pharmacy, Drug Transport and Delivery Research Group, N-9037 Tromsø, Norway

<sup>b</sup>Martin-Luther-University Halle-Wittenberg, Institute of Pharmacy, Department of Pharmaceutics and Biopharmaceutics, Wolfgang-Langenbeck-Str. 4, D-06120 Halle/Saale, Germany

<sup>c</sup>University of Southern Denmark, Department of Physics, Chemistry and Pharmacy, Campusvej 55, DK-5230 Odense M, Denmark

Received: 12 January, 2012; Accepted: 1 March, 2012

### ABSTRACT

This study examines the contribution of a 3-D model in an early development of pectin tablets. The aim of this work was to extract as much information of the compression behavior from as few tablets as possible. Pectins with various degrees of methoxylation (DM) were studied (4%-72%). The compressibility was evaluated using classic “in-die” Heckel and Kawakita analyses in addition to the 3-D modeling. For validation purposes well-known reference materials were included. 3-D modeling applied to data of single tablets yielded some information on their compressibility. When several tablets with different maximum relative densities ( $\rho_{rel, max}$ ) were included, no additional information was obtained through classic evaluation. However, the 3-D model provided additional information through the shape of the 3-D parameter plot. Pectins with a DM  $\geq$  25% consolidated predominantly by elastic deformation similarly to the 3-D parameter plot of pregelatinized starch (PGS). The 3-D analysis also suggests some degree of fragmentation and, for some of the low-methoxylated pectins (DM  $\leq$  10%), viscoelastic deformation. This study showed that by applying 3-D modeling it is possible to differentiate between elastic and viscoelastic materials for tablets with different  $\rho_{rel, max}$  values.

**KEY WORDS:** Degree of methoxylation, compressibility, plastic deformation, elastic deformation, viscoelastic deformation, Heckel equation, Kawakita equation

### INTRODUCTION

Early tablet development focusses on extracting as much information as possible from the smallest number of experiments using

the smallest amounts of material. For this purpose compaction simulators and instrumented tablet presses have proven to be valuable tools (1, 2). In a series of studies we have applied time-resolved force-displacement data obtained from single (or very few) compression(s) on a compaction simulator to analyse the compressibility, i.e., the compression

\*Corresponding author: Ingunn Tho, Department of Pharmacy, University of Tromsø, N-9037 Tromsø, Norway, Tel. +47 776 46632, Fax. +47 776 46151, E-mail: [ingunn.tho@uit.no](mailto:ingunn.tho@uit.no)

behavior, of different tableting excipients (3-7) and binary mixtures (3). Previous studies (6, 7) have employed classic compression parameters derived from the Heckel, Kawakita and Shapiro equations.

The 3-D modelling technique introduced by Picker (8, 9) is an additional tool for estimating the compressibility of powders from time-resolved force-displacement data. In contrast to classic Heckel analysis, this model allows a simultaneous evaluation of force, time and displacement, which in the model are presented as pressure, normalized time, and density. To these data a twisted plane was fitted, characterized by the three parameters:  $d$ ,  $e$  and  $\omega$  (8, 9). Time plasticity  $d$  describes the plastic deformation with respect to time, pressure plasticity  $e$  describes the relationship between density and pressure, while the inverse angle of torsion  $\omega$  is a measure of the materials' elastic recovery in-die (fast elastic decompression) (8, 9). Studies published previously by Picker and Picker-Freyer *et. al.* have shown that even polymers of natural origin of fairly similar compressibility can be distinguished from each other by analysing the three parameters in 3-D parameter plots for several tablets of different maximum relative densities (10-14).

The aim of this study was to test the 3-D model in a development set-up using as few compressions as possible in order to reduce the amount of material required. These materials were chosen to have similar and non-ideal compression properties. Pectin samples with degrees of methoxylation (DM) ranging from 4% to 72% were used. This polysaccharide is an interesting excipient due to its ability to swell and form gels thus providing diffusion and/or erosion controlled release (15, 16). Pectin is also a potential excipient for colon-specific drug delivery due to its specific degradation by colonic enzymes (17-19). Previous studies have shown that pectin grades with very low DM (DM < 10%, also referred to as pectinic acids) were suitable for direct compression, whereas the highest DM grades (DM  $\geq$  50%) did not

form coherent tablets (6, 7). As references for the values obtained through 3-D modelling, some well-described direct compression excipients were included here, namely dibasic calcium phosphate dihydrate (DCPD), microcrystalline cellulose (MCC),  $\alpha$ -lactose monohydrate ( $\alpha$ -LM), and pregelatinized starch (PGS). The aim was to investigate whether compression data obtained from a single tableting event would be sufficient to fully classify the respective materials.

## MATERIALS AND METHODS

### Materials

Two sets of pectin samples with various degrees of methoxylation were tested. The first set was produced from the same demethoxylation process (referred to as same Batch origin) and consisted of DM 25% (26.1%, Batch No. 310707DM25), 35% (34.8%, Batch No. 310707DM35), 40% (41.7%, Batch No. 310707DM40), 50% (51.0%, Batch No. 310707DM50) and 60% (61.6%, Batch No. 310707DM60). The second set was obtained from different original sources with a known DM grade (referred to as different origin) and consisted of DM 4% (Pectin classic AU-L 049/01, Batch No. 0106214), 5% (4.1%, Batch No. 130807DM5), 10% (8.0%, Batch No. 200807DM10) and 72% (Pectin classic CU 202, Batch No. 0810679). The pectin grade with DM 4% originated from apple pomace, the rest were extracted from citrus sources. All samples had been produced by demethoxylation of a high methoxylation (HM) sample. The various pectin grades were donated by Herbstreith & Fox GmbH, Germany. Information on particle size and morphology of the pectin samples has been reported previously (6). Dibasic calcium phosphate dihydrate (DCPD) (Emcompress<sup>®</sup>, Batch No. 905003, JRS Pharma, Germany),  $\alpha$ -lactose monohydrate ( $\alpha$ -LM) (Spherolac<sup>®</sup> 100, Batch No. 907012, Meggle Pharma, Germany), microcrystalline cellulose (MCC) (Avicel<sup>®</sup> PH 102, Batch No. 907014, FMC biopolymer, Belgium), and pregelatinized starch (PGS) (Starch 1500<sup>®</sup>, Batch No. IN 509959, Colorcon,

United Kingdom) were donated by their respective manufacturers and applied as reference materials.

## Powder characterization

### *Apparent particle density*

The apparent particle densities of the pectin samples were determined according to a method developed by Picker and Mielck (20). This method is valid for swellable substances and involves the determination of the apparent particle density when only tightly bound water is present (i.e., at low relative humidity (RH) after the gas purge cycles in the helium densitometer). The apparent particle density at the actual (higher) RH was corrected by adding the apparent particle density of free additional water.

### *Moisture content as the result of varying relative humidity*

The powders were dried at 60°C for 24 hours and brought to room temperature above phosphorus pentoxide (dry material). Samples of approximately 1 gram of the different grades of pectins were accurately weighed and the amount of moisture up-take were recorded gravimetrically by equilibrating over saturated salt solutions of 32% and 43% RH, respectively, until constant mass was obtained (Mettler AE163, Mettler Instrumente AG, Greifensee-Zürich, Switzerland,  $d$ -value 0.01 mg). The moisture content was calculated as the percentage of the dry material. Measurements were made in duplicate.

## Powder compression

### *Powder compression in a compaction simulator*

In the first part of the study a compaction simulator (21) (Schmidt ServoPress 450 Schmidt Technology GmbH, St. Georgen, Germany and compaction module IBR, Waldkirch, Germany) equipped with 11 mm flat-faced punches was used to compress the powder samples. The lower punch was

stationary during the compression and the upper punch moved at a constant speed of 10 mm/second (saw-tooth profile). The punch displacement data were corrected for elastic punch-to-punch deformation (21). Prior to each compression, the punch and die surfaces were lubricated with a 5% suspension of magnesium stearate in acetone. The powder samples were equilibrated at a RH of  $32 \pm 2\%$  (above a saturated magnesium chloride solution), which reflected the conditions of the room. A mass of  $450 \text{ mg} \pm 1 \text{ mg}$  powder was accurately weighed (Sartorius CP225D, Sartorius AG, Göttingen, Germany,  $d$ -value 0.01 mg) and manually poured into the die. Each compression was performed to a maximum pressure corresponding to a maximum relative density ( $\rho_{rel, max}$ ) of  $0.850 \pm 0.005$  (“in-die” porosity of  $0.150 \pm 0.005$ ). Time-resolved force and displacement data were collected for further calculations.

### *Powder compression in an instrumented single punch (eccentric) tablet press*

In the second part of the study an instrumented single punch (eccentric) tablet press (EK0/DMS, No. 1.0083.92, Korsch GmbH, Berlin, Germany) equipped with 11 mm flat-faced punches (Ritter Pharma-Technik GmbH, Hamburg, Germany) was used to compress the powder samples. The experiments were performed in an air-conditioned room at  $20 \pm 2^\circ\text{C}$  and  $43 \pm 3\%$  RH. The displacement of the punches was measured using an inductive transducer (W20 TK, Hottinger Baldwin Messtechnik, Darmstadt, Germany) and corrected for elastic deformation of the punches and the machine. The filling depth was held constant at 13 mm and the production rate was 10 tablets/minute. Due to the construction of the machine, the punch travel speed is not constant, but follows a sinusoidal function at approximately 20 mm/second at die level, gradually decreasing until hitting the respective powder sample and during the further compression event. A mass of 450.0 mg powder was accurately weighed and manually poured into the die, and one compression cycle was performed without the application of a

lubricant. One tablet was produced at seven to ten various  $\rho_{rel, max}$  values, ranging from approximately 0.68 to 0.99 (variable tablet height). Force, time and displacement data of the upper punch were recorded using a DMC-plus system (Hottinger Baldwin Messtechnik, Darmstadt, Germany) and used in further calculations.

## Compression parameters

### 3-D parameters

For the application of the 3-D model, the three parameters were presented in a 3-D parameter plot, to which a twisted plane was fitted by the least-squares method according to Levenberg-Marquardt (Matlab) (8, 9). The 3-D model is presented in Equation 1 (8, 9):

$$z = \ln\left(\frac{1}{1-D_{rel}}\right) = (t-t_{max}) \cdot (d + \omega \cdot (p_{max} - p)) + (e \cdot p) + (f + d \cdot t_{max}) \quad \text{Eq. 1}$$

where,  $D_{rel}$  = relative density,  $t$  = normalized time,  $p$  = pressure,

$$d = \frac{\partial \ln\left(\frac{1}{1-D_{rel}}\right)}{\partial t} \quad e = \frac{\partial \ln\left(\frac{1}{1-D_{rel}}\right)}{\partial p} \quad f = \ln\left(\frac{1}{1-D_{rel}}\right)$$

$t_{max}$  = normalized time at maximum pressure,  $p_{max}$  = maximum pressure, and  $\omega$  = twisting angle at  $t_{max}$ .

The plane is twisted at  $t = t_{max}$ . The time plasticity  $d$ , the pressure plasticity  $e$ , and the fast elastic decompression, i.e. the inverse of  $\omega$ , were calculated. Compression data higher than 50% of the maximum pressure were used for the curve fitting.

### Heckel parameter

The Heckel equation (22, 23) is based on the assumption that powder compression follows first-order kinetics with the inter-particulate pores as the reactant and the densification of the powder bed as the product. The yield pressure ( $YP$ ) of the material,  $YP = 1/k$ , was

derived from the linear part of the Heckel profile according to Equation 2 (22, 23):

$$\ln\left(\frac{1}{E}\right) = kP + A \quad \text{Eq. 2}$$

where,  $E$  is the porosity of the compressed powder bed at applied pressure  $P$ , and  $k$  and  $A$  are constants.

The reciprocal of the slope ( $k$ ) of the linear part of the compression phase was calculated by linear regression in the interval 20% - 80% of the maximum pressure ( $r^2 > 0.998$ ). In general  $YP$  represents the propensity of a material to consolidate by plastic deformation, even though measurements were made “in-die” and are thus considered to reflect both plastic and elastic deformation, and strain hardening (24-30).

### Kawakita parameters

The Kawakita equation (31) assumes that particles subjected to a compressive load in a confined space are considered to be a system in equilibrium at all stages of compression. Consequently, any further volume reduction depends on a volume (porosity) term and pressure. The linear form of the Kawakita equation is presented in Equation 3 (31):

$$\frac{P}{C} = \frac{1}{ab} + \frac{P}{a} \quad \text{Eq. 3}$$

where,

$$C = \frac{V_0 - V}{V_0} = \frac{H_0 - H}{H_0} \quad \text{Eq. 4}$$

$P$  is the applied pressure, and  $C$  is the degree of volume reduction (26, 31), which is equivalent to the engineering strain of the particle bed (32, 33), thus being related to volume or bed height at pressure zero ( $V_0, H_0$ ) and pressure  $P$  ( $V, H$ ).

In the present study,  $H_0$  was set at approximately 0.05 kN corresponding to

approximately 0.6 MPa due to the signal noise. The slope ( $1/a$ ) of the linear part of the compression phase was calculated by linear regression from 20-80% of the maximum pressure ( $r^2 > 0.996$ ). By extrapolating the linear regression line,  $1/ab$  was found at the intercept with the y-axis. The Kawakita  $a$  parameter is commonly interpreted as a constant representing the initial porosity ( $E_0$ ) (26, 31), which corresponds to the total degree of volume reduction for the bed of particles (34). The Kawakita  $b$  parameter is a constant inversely related to the yield strength of the particles (34).

## RESULTS AND DISCUSSION

### 3-D modelling of compression data obtained at similar $\rho_{rel, max}$

All powders were compressed using a compaction simulator to a  $\rho_{rel, max}$  of 0.85 (i.e. “in-die” porosity 0.15). A 3-D parameter plot of the various pectin grades and reference materials is presented in Figure 1, which shows the spread of the different materials.

As expected, the reference materials

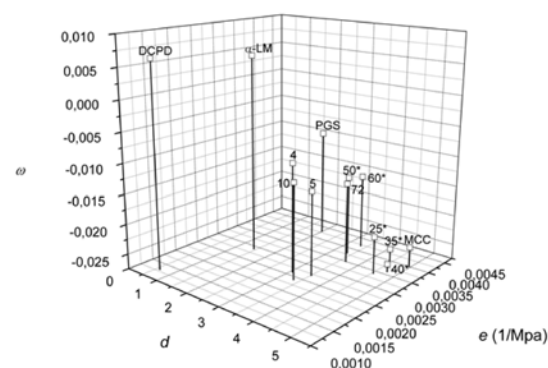


**Figure 1** 3-D parameter plot of various pectin grades and reference materials at a maximum relative density ( $\rho_{rel, max}$ ) of 0.85. The numbers represent the degree of methoxylation (DM) of each pectin sample, and the reference materials are referred to with the following abbreviations: DCPD: Dibasic calcium phosphate dihydrate, MCC: Microcrystalline cellulose,  $\alpha$ -LM:  $\alpha$ -lactose monohydrate, and PGS: Pregelatinized starch. \* From same origin.

representing reasonably different compressibilities showed the most extreme values. Among the reference materials, DCPD showed the lowest values for time plasticity  $d$  and pressure plasticity  $e$  ( $d = 0.60$ ,  $e = 0.0013$ ) and the highest  $\omega$  value (0.0064). Except for a slightly lower  $e$  value, the other parameter values were of the same order of magnitude as previously published data obtained from a linear rotary tableting machine replicator Presster mimicking a Fette 2090 and a Manesty Betapress, respectively (35). Low time plasticity indicated that DCPD was slowly deforming and the low pressure plasticity that a high pressure was needed for the deformation. In addition, no fast elastic decompression was present as indicated by the positive  $\omega$  value. This is consistent with DCPD being known as an extensively fragmenting material (36, 37).  $\alpha$ -LM displayed higher  $d$  and  $e$  values ( $d = 1.4$ ,  $e = 0.0029$ ) compared to DCPD, higher values of both the time plasticity and the pressure plasticity suggested a faster deforming material with less need of a high pressure to deform. As the  $\omega$  value was of the same order of magnitude as DCPD, no significant fast elastic decompression took place in  $\alpha$ -LM either. This is consistent with the literature where  $\alpha$ -LM is described as brittle with low amounts of plastic deformation (38, 39). The highest  $d$  value was found for MCC (5.0), which also showed the lowest  $\omega$  value (-0.024) and a relatively high  $e$  value (0.0040).

It is apparent that the compressibility of MCC was fundamentally different from DCPD with high time plasticity and high pressure plasticity in combination with a negative  $\omega$  value. Thus, MCC was identified as a fast and easily deforming material even at low pressures. This conforms with previous reports in the literature where MCC is described as a predominantly plastically deforming material (40, 41). The fast elastic decompression  $\omega$  was in the same range as previously reported using a rotary press simulator (Presster), whereas the time plasticity  $d$  and the pressure plasticity  $e$  values in the present study differed considerably from values reported previously in the literature (35).

However, it should be noted that MCC of two different particle sizes were used (Avicel® PH 102 in the current study and Avicel® PH 101 previously (35)). For PGS, the pressure plasticity was of the same order of magnitude as MCC, whereas the time plasticity and the fast elastic decompression were in the middle range compared to the other reference materials. It deformed more slowly than MCC and required a higher pressure in order to fragment and/or deform. In general, PGS is known to have elastic deformation components, but still being suitable as a direct compression excipient (13).

Comparing the compressibility of MCC and PGS, surprisingly MCC had a higher fast elastic decompression (lower  $\omega$  value) than PGS. It is reasonable to assume that the observation is related to the 3-D modelling technique using only data at pressures higher than 50% of the maximum pressure (8). Thus, in the case of MCC, the elasticity at high pressures is put forward even though its total elastic recovery has been reported to be significantly smaller than in PGS. By comparing the results from the compaction simulator making a saw-tooth profile with literature data from a rotary press or a single punch eccentric press, it is important to keep in mind that the displacement functions particularly in the higher pressure ranges are different. Hence, the various compression parameters will be influenced (42), and consequently, compression parameters can only be compared when the tablets have been produced on tablet presses with similar displacement functions. Even then differences can be expected. Bateman *et. al.* (43) showed that in a pressure range of 50-200 MPa, the mean yield pressure could differ more than 10% for spray-dried lactose compressed using different compaction simulators.

As all reference materials were characterized according to their well-known compression behaviors, it was interesting to study the pectin samples in more detail. The tested pectin samples were divided into three groups in the 3-D parameter plot (Figure 1), the pectinic acids (DM 4%, DM 5% and DM 10%), the

low-methoxylated (LM) pectins (DM 25%, DM 35% and DM 40%), and the high-methoxylated (HM) pectins (DM 50%, DM 60% and DM 72%). The LM and HM pectins were located between PGS and MCC with respect to time plasticities  $d$ , with the LM pectins closer to MCC. This suggests that LM pectins were most deformable among the pectin samples and showed the highest fast elastic decompression. The pectinic acids indicated slightly lower pressure plasticities  $e$  and slightly higher  $\omega$  values compared to the other pectins. It might, therefore, be suggested that they exhibited some propensity to fragment. However, compared to DCPD the fragmentation propensity was low. The HM pectins showed higher pressure plasticities  $e$ , making them more easily deformable compared to the pectinic acids. It is interesting to note that the pectinic acids produced tablets of adequate mechanical strength, whereas the HM pectins did not produce homogenous tablets in any way. This is consistent with previous findings where the tensile strength of pectinic acid tablets was around 2-3 MPa (6, 7). These studies showed that the degree of methoxylation was the most prominent factor influencing the compressibility, not the particle size nor its shape. It should be noted that pectin particles are fibrous and have an irregular shape, and that the D90-values were around 220  $\mu\text{m}$  for all the samples, except for the samples of  $\text{DM} \leq 10\%$  that had lower particle sizes (6).

The results obtained from a single tablet compression (one  $\rho_{rel, max}$ ) have shown that the 3-D modelling technique can be used to classify pectin powders of various grades into different groups and show major differences in compressibility. The next step in this study was to examine several  $\rho_{rel, max}$  using the 3-D model to investigate if additional information could be obtained by investigating more tablets.

### 3-D modelling of compression data obtained at various $\rho_{rel, max}$

All materials were compressed on an instrumented single punch (eccentric) tablet press to various  $\rho_{rel, max}$  values ranging from 0.68 to 0.997, as shown in Table 1.

**Table 1** Compression parameters from Heckel, Kawakita and 3-D model analyses and apparent particle densities for pectin grades of various degrees of methoxylation (DM). The shaded rows represent the maximum intervals of relative density shown in Figure 2b.

Sample pectin DM (%)	Apparent particle density (g/cm <sup>3</sup> )	Maximum relative density, $\rho_{rel, max}$ (-)	YP (Mpa) (-)	a (-)	1/b (Mpa)	d (-)	e (1/MPa)	$\omega$ (-)
4	1.6611	0.68	107	0.48	22.5	0.3328	0.003	0.007
		0.70	109.2	0.49	24.3	0.3815	0.003	0.006
		0.74	115.6	0.52	26.8	0.5122	0.003	0.006
		0.77	121.1	0.54	29.8	0.684	0.003	0.005
		0.78	118.2	0.54	27.2	0.7575	0.003	0.004
		0.83	119	0.57	31	1.0814	0.003	0.003
		0.87	121.8	0.59	35.4	1.5237	0.003	0.003
		0.90	123	0.6	38.6	1.8237	0.003	0.003
5	1.5987	0.92	125.9	0.61	41.9	2.3461	0.003	0.002
		0.68	66.5	0.51	10.5	0.4052	0.005	0.009
		0.77	73.7	0.56	14.9	0.7719	0.005	0.005
		0.82	-	-	-	1.1462	0.005	0.002
		0.89	80.8	0.62	21.8	1.7536	0.004	0.004
		0.90	80.6	0.63	20.5	1.7083	0.003	0.006
		0.93	80.1	0.64	21.4	2.5053	0.004	0.002
		0.94	81	0.64	22.4	2.7948	0.003	0.003
10	1.6045	0.97	79.3	0.65	25.1	3.9889	0.003	0.001
		0.97	78.8	0.66	23.8	4.646	0.003	0
		0.99	76.3	0.66	24.4	7.2341	0.002	-0.01
		0.73	74.9	0.51	14.7	0.5795	0.005	0.004
		0.76	78.6	0.52	17.5	0.6988	0.005	0.003
		0.80	82.1	0.55	20	0.9044	0.004	0.003
		0.87	85.3	0.61	18.8	1.4986	0.003	0.004
		0.89	89.1	0.59	27.6	1.6773	0.004	0.002
25 <sup>a</sup>	1.5607	0.93	86.6	0.63	22	2.4897	0.003	0.003
		0.95	86.9	0.63	23.4	2.838	0.003	0.003
		0.95	85.2	0.64	23.3	2.9611	0.003	0.002
		0.98	84.7	0.64	24.6	4.4903	0.003	0
		0.996	83.1	0.65	25.6	9.6275	0.002	-0.011
		0.71	54.2	0.6	7.5	0.5059	0.004	0.012
		0.77	60.5	0.62	9.2	0.7658	0.004	0.01
		0.82	64.6	0.64	10.2	1.0296	0.004	0.009
35 <sup>a</sup>	1.561	0.87	68.4	0.66	11.7	1.5955	0.004	0.006
		0.91	70.7	0.67	13.2	2.006	0.004	0.008
		0.95	72	0.69	14.2	3.1286	0.004	0.005
		0.97	73.1	0.68	15.8	4.4648	0.004	0
		0.97	72.1	0.69	14.8	5.1305	0.004	0
		0.99	71.5	0.69	16.2	8.3405	0.004	-0.013
		0.996	71.5	0.7	15.6	12.3568	0.003	-0.027
		0.68	49.8	0.59	8.9	0.3997	0.005	0.0127
40 <sup>a</sup>	1.543	0.73	53.8	0.62	9.5	0.6026	0.005	0.0103
		0.80	59.7	0.65	11.7	0.9672	0.004	0.008
		0.88	63.7	0.67	13.4	1.6501	0.004	0.006
		0.93	67.4	0.69	14.2	2.4041	0.004	0.007
		0.94	67.3	0.69	13.9	2.8256	0.005	0.003
		0.96	67.9	0.7	14.1	3.6987	0.004	0.004
		0.96	68.4	0.69	14.6	3.5859	0.004	0.006
		0.98	68.2	0.7	15	5.7195	0.004	0
40 <sup>a</sup>	1.543	0.997	67.9	0.7	14.5	13.8037	0.003	-0.035
		0.69	51.6	0.6	8.5	0.4613	0.005	0.0118
		0.73	54.8	0.63	9.6	0.6432	0.005	0.0104
		0.83	61.1	0.67	11.9	1.2457	0.004	0.007
		0.90	64.4	0.69	13.4	1.8906	0.004	0.008
		0.93	65.4	0.69	13.7	2.4799	0.004	0.007
		0.95	66.4	0.7	14.7	3.3551	0.004	0.006
		0.96	66	0.7	14.7	3.6868	0.004	0.005
0.98	66.1	0.7	15.3	5.0036	0.004	0		
0.98	65.7	0.7	15.5	4.9261	0.004	0.003		

Table 1 Cont.

Sample pectin DM (%)	Apparent particle density (g/cm <sup>3</sup> )	Maximum relative density, $\rho_{rel, max}$	YP (Mpa)	a (-)	1/b (Mpa)	d (-)	e (1/Mpa)	$\omega$ (-)
50 <sup>a</sup>	1.5653	0.75	58.3	0.54	11.1	0.5271	0.004	0.0102
		0.89	73.3	0.63	15.1	1.4441	0.004	0.009
		0.92	76.3	0.64	15.4	1.9167	0.004	0.009
		0.93	76.7	0.64	15.8	2.0835	0.004	0.008
		0.94	77.6	0.65	15.4	2.3471	0.004	0.008
		0.94	77.7	0.65	15.9	2.3652	0.004	0.008
		0.95	77.8	0.65	16.7	2.8536	0.004	0.007
		0.97	78.9	0.66	16.3	3.5033	0.004	0.006
		0.97	77.5	0.66	17.1	3.667	0.004	0.005
60 <sup>a</sup>	1.532	0.74	45.1	0.51	7.7	0.4631	0.007	0.0157
		0.84	52.7	0.56	9.9	0.9455	0.006	0.0122
		0.94	53.4	0.56	14.1	2.2131	0.007	0.006
		0.98	60.8	0.63	14.9	4.3082	0.007	0
		0.99	60.2	0.63	15.2	6.5677	0.007	-0.016
		0.996	59.7	0.63	15.4	10.8103	0.008	-0.046
72	1.5592	0.86	118.8	0.57	23.8	1.1473	0.003	0.006
		0.87	120.2	0.59	25.6	1.2953	0.003	0.005
		0.89	123.6	0.59	27.5	1.5835	0.003	0.005
		0.91	124.7	0.61	28.6	1.7787	0.003	0.005
		0.91	123	0.62	34.8	1.8739	0.003	0.005
		0.93	122.4	0.61	31.3	2.2791	0.003	0.004
		0.96	121.5	0.62	30.6	3.3235	0.003	0.002
		0.97	124.1	0.62	33.4	5.0576	0.003	0
		0.99	124.7	0.62	34.7	8.4631	0.002	-0.01

<sup>a</sup>from same batch origin

Due to the different location of the compaction equipment, the experiments were carried out at a higher RH ( $43 \pm 3\%$ ) compared to those on the compaction simulator ( $32 \pm 2\%$ ). The effect of the different relative humidity on the moisture content of the samples was determined. As expected, for all the samples the difference in moisture content was low, less than 3% at the higher RH (Table 2), and the relationship between the samples remained unchanged. For the reference excipients, the differences in the absolute moisture contents were also low (less than 10% for the Starch 1500<sup>®</sup> used, less than 5% for the others).

**Table 2** Water content of pectin powder samples at the different relative humidities (RH) of the compaction experiments

Material	Water content (%)	
	32 ± 2% RH	43 ± 3% RH
Pectin DM 4%	n/a	n/a
Pectin DM 5%	7.19 ± 0.37	9.24 ± 0.30
Pectin DM 10%	7.17 ± 0.45	10.08 ± 0.47
Pectin DM 25%	7.63 ± 0.52	9.89 ± 0.44
Pectin DM 35%	7.53 ± 0.35	9.37 ± 0.23
Pectin DM 40%	8.13 ± 0.12	10.25 ± 0.00
Pectin DM 50%	9.89 ± 0.16	12.67 ± 0.11
Pectin DM 60%	9.36 ± 0.75	11.95 ± 0.78
Pectin DM 72%	n/a	n/a

<sup>a</sup> From same origin, n/a Not available

The 3-D parameter plot (Figure 2a) shows that the tested pectin samples formed three clusters distinguished by the size of the  $e$  values, e.g. the pressure plasticities. However, the compositions of the groups were slightly changed compared to the grouping seen in Figure 1. The highest pressure plasticities ( $e$  values) were found for DM 60%, suggesting an easily deforming material at low pressures, whereas DM 4%, DM 10% and DM 72% constituted the group with the lowest  $e$  values.

To study the compressibility of the individual samples in more detail, the 3-D parameter plot was restricted to the similar  $\rho_{rel, max}$  intervals for all samples. Figure 2b shows the 3-D parameters for compacts with  $\rho_{rel, max}$  from 0.68 to 0.90. For all pectin grades the time plasticities increased considerably with increasing powder densification. Among the three clusters identified above, the group with the lowest  $e$  values (DM 4%, DM 10% and DM 72%) displayed flat curves compared to the other profiles (Figure 2b). However, most of the other pectin samples showed decreasing  $\omega$  values in combi-



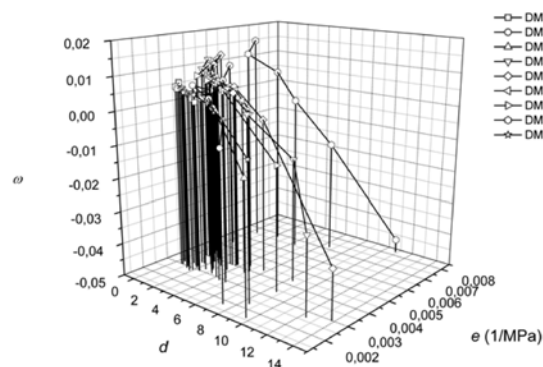


**Figure 2a** 3-D parameter plot of various pectin grades at various maximum relative densities ( $\rho_{rel,max}$ ) ranging from 0.68 to 0.997. \* From same origin.

nation with decreasing  $e$  values, which indicates some brittleness (44). For pectin with  $DM \geq 25\%$  the fast elastic decompression increased with higher  $\rho_{rel,max}$ , as decreasing  $\omega$  values suggested. It is also interesting to note that the  $\omega$  values were positive whereas data derived from a Presster compaction simulator equipped with different compression wheels yielded negative  $\omega$  values (35). It would therefore appear reasonable to assume that this difference is a result of the different displacement functions and punch velocities for the machines.

Again, for validation purposes the results obtained for the pectin samples were compared with reference materials from the literature (44). For clarity, values for three randomly chosen pectin grades (DM 4%, DM 25% and DM 60%, Table 1) and values for four selected reference materials from Picker (44) (DCPD, MCC,  $\alpha$ -LM and PGS) were plotted at similar  $\rho_{rel,max}$  intervals (Figure 3). Detailed information on the compressibilities for the different reference materials have been discussed previously in detail by Picker (44). Among the pectin grades, DM 4% showed a relatively flat profile with lower pressure plasticity and higher fast elastic decompression compared to MCC. The profile has similarities to the curve progressions for viscoelastic materials such as

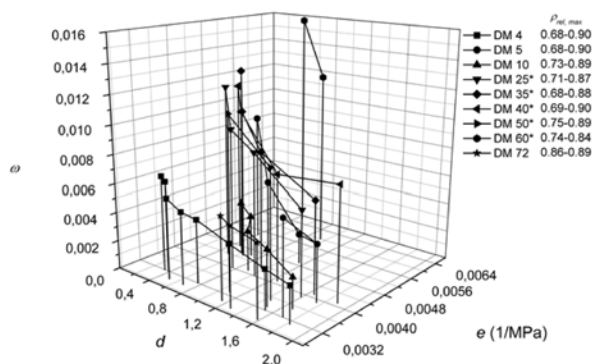


**Figure 2b** 3-D parameter plot of various pectin grades at similar maximum relative density ( $\rho_{rel,max}$ ) intervals. \* From same origin.

cellulose acetate (CAC) (10, 44) and sodium carboxy-methylcellulose (NaCMC) (44). Hence, DM 4 % seemed to display some degree of viscoelastic behaviour. The highest  $e$  values were observed for DM 60% (Figure 3), which suggested this pectin grade to be easily deforming at low pressures. For DM 25% the curve progression was very similar to PGS (Figure 3), indicating tendencies to undergo elastic deformation. The  $e$  values were slightly lower for DM 25% compared to PGS (0.0040 (Table 1) vs. 0.0049 at  $\rho_{rel,max}$  0.77 (44)).

The difference in pressure plasticity suggested that pectin DM 25% would require slightly higher pressure than PGS in order to deform. A comparison of the  $d$  values at a  $\rho_{rel,max}$  of 0.77 showed somewhat higher values for DM 25% (0.7658, Table 1) compared to PGS (0.5240, (44)). This suggested a slightly faster deformation in pectin compared to PGS. At  $\rho_{rel,max}$  below 0.80 the  $\omega$  values of DM 25% were slightly higher than for PGS, but above this  $\rho_{rel,max}$  DM 25% showed the lowest  $\omega$  values.

It is interesting to compare pectins to other polysaccharides. Both carrageenans and chitosans have been reported to consolidate predominantly by plastic deformation with a

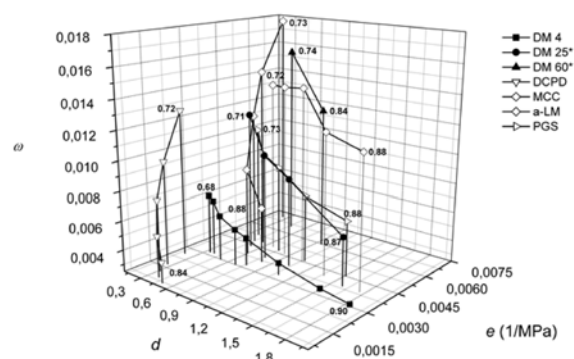


**Figure 3** 3-D parameter plot of three selected pectin grades (DM 4%, DM 25% and DM 60%) and reference materials (dibasic calcium phosphate dihydrate (DCPD), microcrystalline cellulose (MCC),  $\alpha$ -lactose monohydrate ( $\alpha$ -LM), and pregelatinized starch (PGS)) published by Picker (44). For each sample the maximum relative density ( $\rho_{rel, max}$ ) intervals are given. \* From same origin.

simultaneous fast elastic decompression followed by elastic recovery “out-of-die” (10–12). For alginates, the type of salt influences the compression behavior, for sodium alginates

elastic deformation is reported to dominate, whereas potassium alginates are less elastic and show some brittleness (14). Figure 3 shows that the pectins are more similar to alginates than to carrageenans or chitosans.

#### Acquired information from one single tablet vs. several tablets at several $\rho_{rel, max}$

Evaluation of one tablet of a given  $\rho_{rel, max}$  of each material through the 3-D model can differentiate between the pectins based on their plastic deformation and fast elastic decompression. Adding more tablets of different  $\rho_{rel, max}$  to the 3-D model resulted in a separation of the pectin samples into three groups. However, more importantly additional information on the elastic behaviour of a material was obtained through the shape of the profiles. On the contrary, classic equations such as the Heckel and Kawakita equations did not provide additional information with more tablets (rather constant parameter values, Table 1). More detailed, sequential handling of the

data of the single tablets, as suggested by Nordström *et al.* (32) and Klevan *et al.* (45, 46), may provide additional information for the onset phase of pressure, e.g. particle rearrangement. These phenomena were not captured by the 3-D model which is exclusively based on data from the higher pressure part of the curves. However, by examining several tablets made at different maximum pressures using 3-D analysis, slight differences in viscoelastic behavior were observed, could not be fully discerned from the analysis of a single tablet.

#### CONCLUSION

In this study the 3-D model was tested in a development set-up using as few tablets as possible to characterize the compressibility of materials of similar and non-ideal compression properties. The results show that pectin powders of various degrees of methoxylation (DM), ranging from 4% to 72%, were separated into clusters in a 3-D parameter plot based on their major deformation properties. By analysing the results from a single compression for each material, it was possible to differentiate between the compressibilities of the three clusters: pectinic acids (DM < 10%), LM and HM pectins. The results confirmed that LM pectins exhibit the highest degrees of plastic deformation and fast elastic decompression. Further, pectinic acids were found to possess a certain degree of fragmentation and the HM pectins were more easily deformable than the pectinic acids, although they did not form coherent tablets. If several compacts of the same material at various maximum relative densities ( $\rho_{rel, max}$ ) were produced, no additional information could be obtained with the classic equations (Heckel and Kawakita). However, 3-D modelling provided more detailed information on the elastic behaviour of the materials through the shape of the density profiles. For early tablet development, it is suggested to begin by using the 3-D model on a single tablet followed by validation using classic compression equations. If the material is viscoelastic, it is recommended to apply 3-D modelling to

several tablets of different maximum relative densities to achieve the full potential of the model. However, adding more tablets to compression studies needs to balance material consumption and the benefit of the additional studies.

## ACKNOWLEDGEMENTS

The authors would like to thank Ritter Pharma-Technik GmbH, Hamburg, Germany, for donation of punches both to the tablet press and the compaction simulator.

## REFERENCES

- Celik, M, Marshall, K, Use of a compaction simulator system in tableting research. I. Introduction to and initial experiments with the system. *Drug Dev Ind Pharm*, 15(5): 759-800, 1989.
- Rubeinstein, MH, Compaction simulators - Industrial tool or research toy? *Eur Pharm Rev*, September: 25-33, 1996.
- Haware, RV, Tho, I, Bauer-Brandl, A, Application of multivariate methods to compression behavior evaluation of directly compressible materials. *Eur J Pharm Biopharm*, 72(1): 148-155, 2009.
- Haware, RV, Bauer-Brandl, A, Tho, I, Comparative evaluation of the powder and compression properties of various grades and brands of microcrystalline cellulose by multivariate methods. *Pharm Dev Technol*, 15(4): 394-404, 2010.
- Haware, RV, Tho, I, Bauer-Brandl, A, Multivariate analysis of relationships between material properties, process parameters and tablet tensile strength for alpha-lactose monohydrates. *Eur J Pharm Biopharm*, 73(3): 424-431, 2009.
- Salbu, L, Bauer-Brandl, A, Tho, I, Direct Compression Behavior of Low- and High-Methoxylated Pectins. *AAPS PharmSciTech*, 11(1): 18-26, 2010.
- Salbu, L, Bauer-Brandl, A, Alderborn, G, Tho, I, Effect of degree of methoxylation and particle size on compression properties and compactibility of pectin powders. *Pharm Dev Technol*: In press, DOI: 10.3109/10837450.2010.535831, 2010.
- Picker, KM, A new theoretical model to characterize the densification behavior of tableting materials. *Eur J Pharm Biopharm*, 49(3): 267-273, 2000.
- Picker-Freyer, KM, The 3-D model: Experimental testing of the parameters d, e, and omega and validation of the analysis. *J Pharm Sci*, 96(5): 1408-1417, 2007.
- Picker, KM, "Soft tableting": A new concept to tablet pressure-sensitive materials. *Pharm Dev Technol*, 9(1): 107-121, 2004.
- Picker-Freyer, KM, Carrageenans: Analysis of tablet formation and properties (part II). *Pharm Technol Eur*, 17(9): 32, 34, 36, 38, 40, 42, 44, 2005.
- Picker-Freyer, KM, Brink, D, Evaluation of powder and tableting properties of chitosan. *AAPS PharmSciTech*, 7(3): Article 75, 2006.
- Odeku, OA, Schmid, W, Picker-Freyer, KM, Material and tablet properties of pregelatinized (thermally modified) Dioscorea starches. *Eur J Pharm Biopharm*, 70(1): 357-371, 2008.
- Schmid, W, Picker-Freyer, KM, Tableting and tablet properties of alginates: Characterisation and potential for Soft Tableting. *Eur J Pharm Biopharm*, 72(1): 165-172, 2009.
- Sungthongjeen, S, Pitaksuteepong, T, Somsiri, A, Sriamornsak, P, Studies on pectin as potential hydrogel matrices for controlled-release drug delivery. *Drug Dev Ind Pharm*, 25(12): 1271-1276, 1999.
- Sriamornsak, P, Thirawong, N, Weerapol, Y, Nunthanid, J, Sungthongjeen, S, Swelling and erosion of pectin matrix tablets and their impact on drug release behavior. *Eur J Pharm Biopharm*, 67: 211-219, 2007.
- Ashford, M, Fell, J, Attwood, D, Sharma, H, Woodhead, P, Studies on pectin formulations for colonic drug-delivery. *J Control Release*, 30(3): 225-232, 1994.
- Rubinstein, A, Radai, R, Ezra, M, Pathak, S, Rokem, JS, In-vitro evaluation of calcium pectinate - A potential colon-specific drug delivery carrier. *Pharm Res*, 10(2): 258-263, 1993.
- Sande, SA, Pectin-based oral drug delivery to the colon. *Expert Opin Drug Deliv*, 2(3): 441-450, 2005.
- Picker, KM, Mielck, JB, True density of swellable substances at different relative humidities - A new approach to its determination. *Eur J Pharm Biopharm*, 42(1): 82-84, 1996.
- Klevan, I, Haware, RV, Reichenbach, M, Bauer-Brandl, A. A new tablet press simulator device for extremely accurate measurement of time-resolved forces and displacements based on an electromechanical press. in *Pharmaceutical Sciences World Congress*. 2007. Amsterdam: The Netherlands.
- Heckel, RW, Density-pressure relationships in powder compaction. *Trans Metall Soc Aime*, 221(4): 671-675, 1961.
- Heckel, RW, An analysis of powder compaction phenomena. *Trans Metall Soc Aime*, 221(5): 1001-1008, 1961.
- Duberg, M, Nyström, C, Studies on direct compression of tablets. XVII. Porosity pressure curves for the characterization of volume reduction-mechanisms in powder compression. *Powder Technol*, 46(1): 67-75, 1986.
- Paronen, P, Heckel plots as indicators of elastic properties of pharmaceuticals. *Drug Dev Ind Pharm*, 12: 1903-1912, 1986.

- 26 Patel, S, Kaushal, AM, Bansal, AK, Effect of particle size and compression force on compaction behavior and derived mathematical parameters of compressibility. *Pharm Res*, 24(1): 111-124, 2007.
- 27 Patel, S, Kaushal, AM, Bansal, AK, Mechanistic investigation on pressure dependency of Heckel parameter. *Int J Pharm*, 389: 66-73, 2010.
- 28 Sonnergaard, JM, A critical evaluation of the Heckel equation. *Int J Pharm*, 193: 63-71, 1999.
- 29 Sonnergaard, JM, Impact of particle density and initial volume on mathematical compression models. *Eur J Pharm Sci*, 11: 307-315, 2000.
- 30 Sun, C, Grant, DJ, Influence of elastic deformation of particles on Heckel analysis. *Pharm Dev Technol*, 6: 193-200, 2001.
- 31 Kawakita, K, Lüdde, K-H, Some considerations on powder compression equations. *Powder Technol*, 4(2): 61-68, 1971.
- 32 Nordstrom, J, Klevan, I, Alderborn, G, A Particle Rearrangement Index Based on the Kawakita Powder Compression Equation. *J Pharm Sci*, 98(3): 1053-1063, 2009.
- 33 Nicklasson, F, Alderborn, G, Analysis of the compression mechanics of pharmaceutical agglomerates of different porosity and composition using the Adams and Kawakita equations. *Pharm Res*, 17(8): 949-954, 2000.
- 34 Kawakita, K, Hattori, I, Kishigami, M, Characteristic constants in Kawakita's powder compression equation. *J Powder Bulk Solids Technol*, 1: 3-8, 1977.
- 35 Picker, KM, The 3-D model: Comparison of parameters obtained from and by simulating different tableting machines. *AAPS PharmSciTech*, 4(3): Article 35, 2003.
- 36 McKenna, A, McCafferty, DF, Effect of particle size on the compaction mechanism and tensile strength of tablets. *J Pharm Pharmacol*, 34(6): 347-351, 1982.
- 37 Roberts, RJ, Rowe, RC, The effect of punch velocity on the compaction of a variety of materials. *J Pharm Pharmacol*, 37(6): 377-384, 1985.
- 38 Lerk, CF, Consolidation and compaction of lactose. *Drug Dev Ind Pharm*, 19(17-18): 2359-2398, 1993.
- 39 Vromans, H, Deboer, AH, Bolhuis, GK, Lerk, CF, Kussendrager, KD, Bosch, H, Studies on tableting properties of lactose. II. Consolidation and compaction of different types of crystalline lactose. *Pharm Weekbl Sci*, 7(5): 186-193, 1985.
- 40 David, ST, Augsburger, LL, Plastic flow during compression of directly compressible fillers and its effect on tablet strength. *J Pharm Sci*, 66(2): 155-159, 1977.
- 41 Roberts, RJ, Rowe, RC, The effect of the relationship between punch velocity and particle size on the compaction behaviour of materials with varying deformation mechanisms. *J Pharm Pharmacol*, 38(8): 567-571, 1986.
- 42 Palmieri, GF, Joiris, E, Bonacucina, G, Cespi, M, Mercuri, A, Differences between eccentric and rotary tablet machines in the evaluation of powder densification behaviour. *Int J Pharm*, 298: 164-175, 2005.
- 43 Bateman, SD, Rubinstein, MH, Rowe, RC, Roberts, RJ, Drew, P, Ho, AYK, A comparative investigation of compression simulators. *Int J Pharm*, 49: 209-212, 1989.
- 44 Picker, KM, The 3D model: Explaining densification and deformation mechanisms by using 3D parameter plots. *Drug Dev Ind Pharm*, 30(4): 413-425, 2004.
- 45 Klevan, I, Nordstrom, J, Bauer-Brandl, A, Alderborn, G, On the physical interpretation of the initial bending of a Shapiro-Konopicky-Heckel compression profile. *Eur J Pharm Biopharm*, 71(2): 395-401, 2009.
- 46 Klevan, I, Nordstrom, J, Tho, I, Alderborn, G, A statistical approach to evaluate the potential use of compression parameters for classification of pharmaceutical powder materials. *Eur J Pharm Biopharm*, 75(3): 425-435, 2010.